

Development and Evaluation of Combined Wavelet Based Palmprint Identification System

Atif Bin Mansoor^{a,b,*}, Hassan Masood^b, Mustafa Mumtaz^b and Shoab Ahmad Khan^a

^aCASE, University of Engineering & Technology, Taxila, Pakistan

^bCAE, National University of Science and Technology, H-12, Islamabad, Pakistan

(received July 31, 2009; revised May 3, 2010; accepted May 12, 2010)

Abstract. Palmprint based identification is fairly recent biometric modality gaining popularity due to its traits like user comfort, reliability and easy acquisition. A wavelet based palmprint identification system has been proposed. Euclidean distance based classification is performed using Biorthogonal, Symlet and Discrete Meyer wavelets on 500 palmprints obtained from 50 users for individual and combined features, employing locally developed acquisition platform. An equal error rate (EER) of 0.0217 and genuine acceptance rate (GAR) of 97.12% demonstrate the effectiveness of the combined system.

Keywords: biometrics, palmprint, wavelet transform, distance transform

Palmprint based identification is fast gaining popularity due to user acceptance, ease of acquisition, reliability and uniqueness (Kong *et al.*, 2009). Scanners and pegged systems are used for acquiring the palmprints (Zhang *et al.*, 2004). Scanners are hygienically susceptible while systems with pegs are not user friendly. Different wavelet transforms and their combination for palmprint identification, through developing a user friendly peg free system are being reported here (Fig. 1a).

The system comprises of an enclosed black box, with ring shaped lighting tube for uniform illumination and two flat plates, 14 cm apart. The camera and the light source are fixed on the upper plate while the bottom plate is used to place the hand for image acquisition. As dataset, 10 images from 50 male individuals were collected, resulting in total of 500 images. The age distribution of individuals was between 22 to 56 years, with 80% between 22 to 25 years. SONY DSC W-35 cyber shot camera was utilized for imaging.

The captured palmprint colour images having RGB (red, green, blue) components (Kumar and Zhang, 2006) were changed to hue saturation intensity (HSI) parameters and analyzed by its intensity values (I). The obtained gray level images were normalized and then hysteresis was thresholded to obtain a binarized image. Rotational alignment, incorporated using the second order moments, helped analyze the elongation and eccentricity. Second order statistical moments gave the parameters of best fitting ellipse (Kumar and Zhang, 2006). Ratios between eigen values helped examine the shape whereas direction of elongation was evaluated using the direction of the eigenvector corresponding to the highest eigen value. Subsequently, the offset (θ) between the normal

axis and the major axis of the ellipse was calculated (Fig. 1b). The palmprint was then vertically aligned and further processed to remove noise in the binary image and to evaluate the centre of palmprint.

Five images of each user were utilized for training while the rest five were used for validation. Wavelet families namely Biorthogonal 3.9, Symlet 8 and Demeyer 5 were used to extract the textural information of palmprint images. ROI decomposed into three scales using each wavelet type, and resultantly ten directional details were obtained for each wavelet. The approximation level was ignored and the directional energy in nine detailed levels was calculated. The directional energy in each level was normalized to reduce variation in the gray levels of palmprint images due to illumination variance (Mumtaz *et al.*, 2009; Masood *et al.*, 2008). The energy values computed from each block for the three wavelet types are concatenated to form a feature vector of length 27 for an individual palmprint. The normalized energy of the region of interest (ROI) image block B associated with subband 'a' is given by the formula:

$$E_a = \sum_{u,v \in B} [(\square | f_a(u,v) | \square)] \quad (1)$$

where, u and v are the coordinates of the pixel in consideration and summation indicates the sum of all normalized energies of the particular ROI.

The normalized energy is given as:

$$E = \frac{E_a}{\sum_{a=1}^n E_a} \quad (2)$$

where 'n' is the total number of blocks present in the image.

*Author for correspondence; E-mail: atif-cae@nust.edu.pk

Matching was performed by calculating the Euclidean distance between the input feature vector and template feature vector. The three wavelet types were also analyzed for their individual performance by formulating similar energy based feature vectors of length 27 using 9 levels decomposition. Fig. 1c gives the genuine and imposter distribution for the combined wavelet approach. Fig. 2a, 2b, and 2c give the distribution curves for individual wavelets i.e., Biorthogonal 3.9, Symlet 8 and Demeyer, respectively.

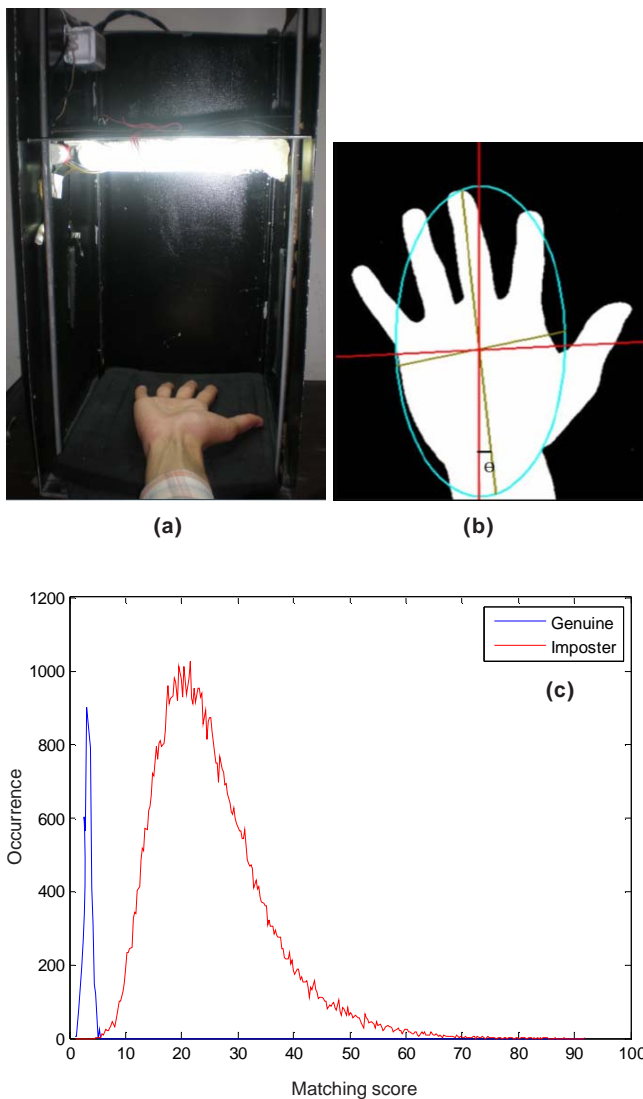


Fig. 1. (a) Image acquisition platform; (b) calculation of alignment of palm by finding offset θ ; (c) genuine and imposter distribution for combined approach.

Figure 3a gives threshold vs FMR and FNMR graph for the three wavelet filters and their combined approach, while Fig. 3b gives corresponding receiver operating curves.

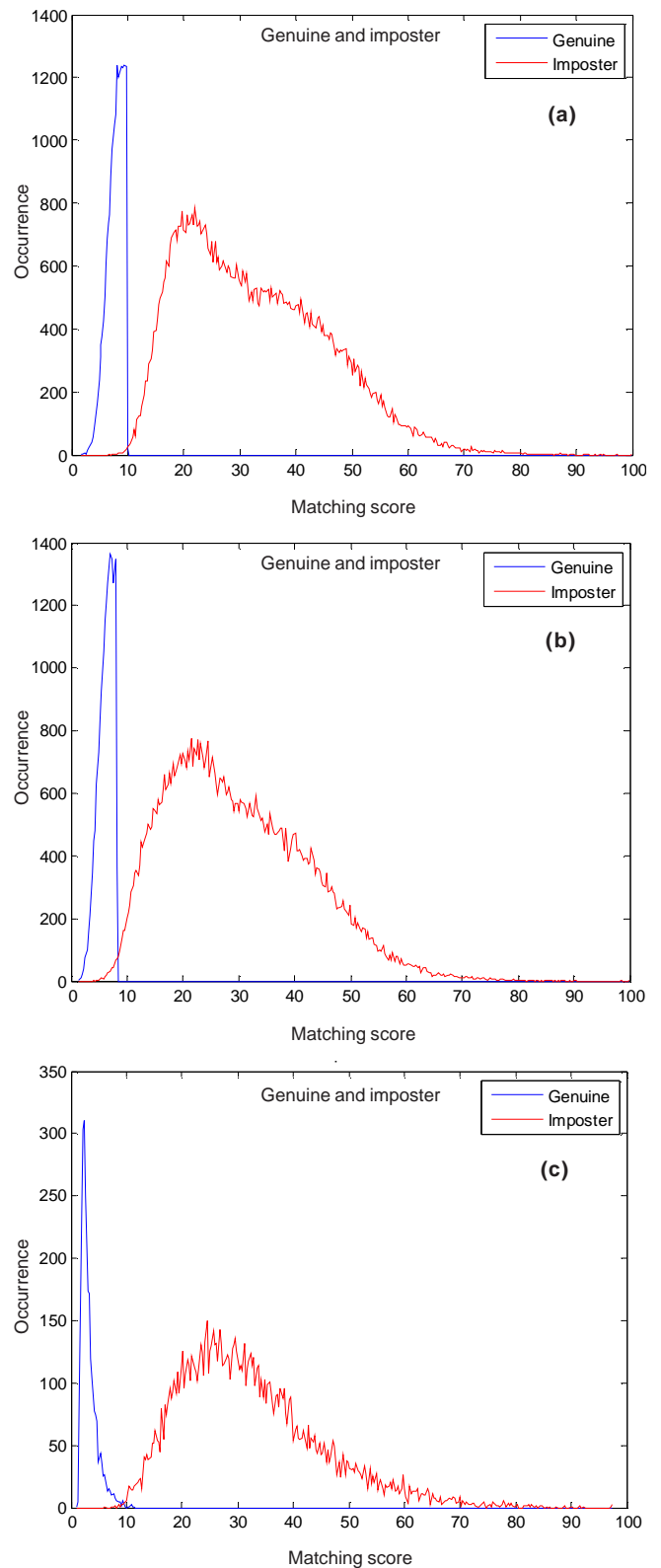


Fig. 2. (a) Genuine and imposter distribution curve for Bior 3.9; (b) genuine and imposter distribution curve for Symlet 8; (c) genuine and imposter distribution curve for Demeyer.

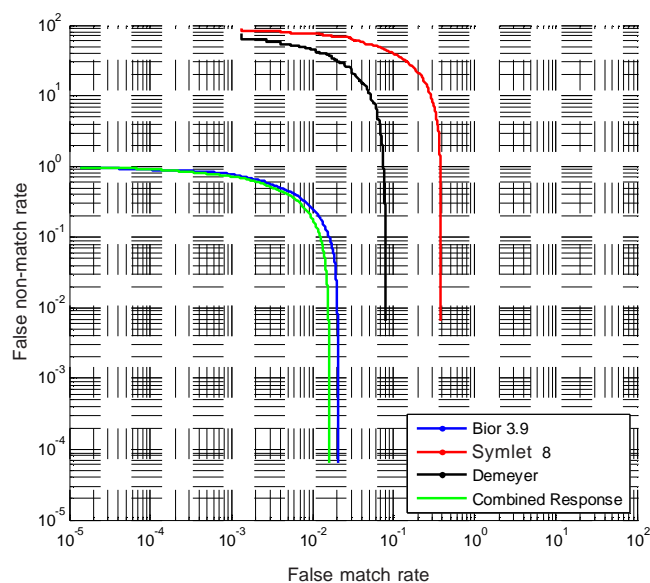
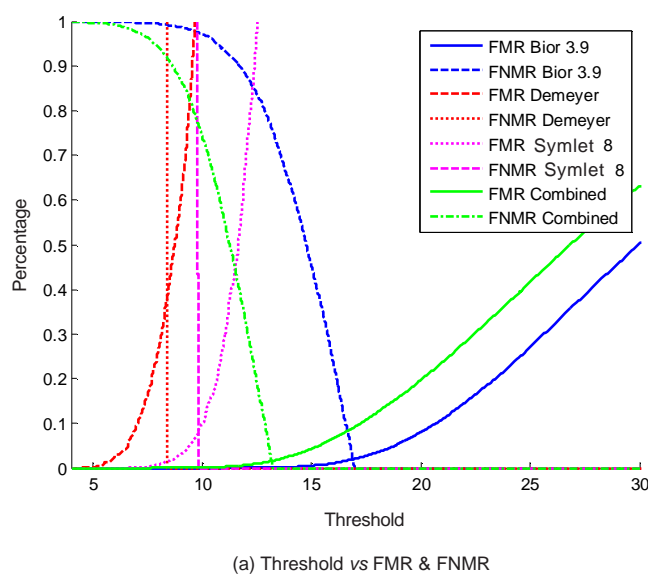


Fig. 3. (a) Threshold vs FMR and FNMR for all the three filters and their combined response; (b) receiver operating curve for all the three filters and their combined response.

Table 1 summarizes the equal error rate, EER, decidability index and genuine acceptance rate (GAR) for different wavelets for their individual and combined performance. The experimental results showed Symlet wavelet kernel to give the best individual result among the three wavelets. The wavelets combination gave GAR of 97.12% and EER of 0.0217, better than individual wavelets as the multi-resolution strength of individuals supplemented each other. Thus, the combination of multiple wavelets achieved significant improvement in the system performance.

Table 1

Wavelet	EER	Decidability index	GAR (%)
Bior 3.9	0.0322	2.6411	76.23
Symlet 8	0.0821	2.6987	84.45
Demeyer	0.3833	2.5677	71.1
Combination	0.0217	3.1275	97.12

Among the three individual wavelet kernels, Bior 3.9 gave the best equal error rate while combined wavelet approach outperformed the individual wavelet feature for the palmprint identification.

References

- Kong, A., Zhang, D., Kamel, M. 2009. A survey of palmprint recognition. *Pattern Recognition*, **42**: 1408-1418.
- Kumar, A., Zhang, D. 2006. Personal recognition using hand shape and texture. *IEEE Transactions on Image Processing*, **15**: 2454-2461.
- Masood, H., Mumtaz, M., Butt, M.A.A., Mansoor, A.B., Khan, S.A. 2008. Wavelet based palmprint authentication system. In: *Proceedings of IEEE International Symposium on Biometrics and Security Technologies, ISBAST*, pp. 1-7.
- Mumtaz, M., Mansoor, A.B., Masood, H. 2009. Directional energy based palmprint identification using non sub-sampled contourlet transform. In: *Proceedings of IEEE International Conference on Image Processing*, pp. 1965-1968.
- Zhang, D., Lu, G., Kong, W.K., Wong, M. 2004. Palmprint authentication technologies, systems and applications. In: *Proceedings of 5th Chinese Conference on Biometric Recognition, SINOBIOMETRICS 2004*, S. Z. Li., J. -H. Lai, T. Tan, G. -C. Feng and Y. Wang (eds.), vol. **3338**, Springer Verlag, Heidelberg, Germany.